

Spectral Efficiency Analysis in Cell-Free Massive MIMO Systems with Zero-Forcing Detector

Pei Liu, Kai Luo, Da Chen, and Tao Jiang

Abstract

This paper investigates the spectral efficiency performance of the cell-free massive multiple-input multiple-output (MIMO) systems employing linear zero-forcing detector. We firstly derive the approximate upper/lower-bound of the achievable uplink rate for the functions of the number of base-station antennas L and the large-scale fading, with the perfect channel state information (CSI) and imperfect CSI, respectively. Those bound results for both cases are not only in the simple unified expressions, but also can degrade into the bound results in the conventional massive MIMO systems. In addition, our obtained bounds in imperfect CSI case degrade into the perfect CSI case when the pilot sequence power becomes infinite. Particularly, the asymptotic analysis shows that the obtained bounds have an asymptotic lower-bound $\frac{\alpha}{2} \log_2 L$ for all cases in cell-free massive MIMO thanks to the extra *distance diversity* offered by massively distributed antennas, which the path-loss factor $\alpha > 2$ except the free space environment. In other words, cell-free massive MIMO has huge potential of spectral efficiency than conventional massive MIMO with the asymptotically tight bound $\log_2 L$. Finally, the above mentioned results are verified via the Monte-Carlo simulations.

Index Terms

Spectral efficiency, cell-free massive MIMO, upper/lower-bound, *distance diversity*, CSI.

I. INTRODUCTION

To meet the ever-increasing demand for high data rate, there is an urgent need to improve the spectral efficiency (SE) [1]. In this regard, massive multiple-input multiple-output (MIMO)

The authors are with the School of Electronic Information and Communications, Huazhong University of Science and Technology, Wuhan 430074, China (e-mail: peil@hust.edu.cn; kluo@hust.edu.cn; chenda@hust.edu.cn; Tao.Jiang@ieee.org).

technology, which deploys hundreds of antenna elements at the base-station (BS) side to provide data traffic to tens of users simultaneously at the same time-frequency resource [2], has been at the forefront of the future wireless communication architecture [3] thanks to its high SE characteristic provided by the massive array [4–6]. Consequently, the conventional massive MIMO research that routinely assumes the BS antennas are placed at a given and fixed location in a centralized manner, which brings the benefits of performance analysis especially for the SE [7, 8]. In addition, a diametrically opposite point is about distributing the BS antennas into a area uniformly. The seminal work [9] shows that this distributed antenna system can cover dead spots effectively. Hence, this topic has also attracted enormous attentions from academia and industry in the past decades. The relative research reflects that distributed antenna system has the ability of improving cell coverage, saving power, offering more spatial resources, shortening the average access distance between user and BS, and etc [10, 11]. Naturally, it is therefore of paramount importance to fuse the merits of conventional massive MIMO systems and distributed antenna systems and, thereafter, aim to satisfy the future communication system performance requirement.

In recent years, cell-free massive MIMO systems [12] (also referred to as distributed massive MIMO systems [13] and etc), in which massive BS antennas are distributed over a wide area to serve a amount of users, have obtained a great deal of interest since its possesses the mixed characteristic of the above mentioned two systems. Essentially, based on the classic work performed by Telatar [14], it is obvious that the statistical characterization of the instantaneous channel correlation matrix is vital importance to the SE performance. In conventional massive MIMO, since the served user has the uniform and identical large-scale fading coefficient to all centralized BS antennas, the corresponding channel correlation matrix follows the Wishart distribution which its statistical properties have been largely and extensively characterized [15], that the corresponding SE analysis has been well investigated [5, 16]. However, in cell-free massive MIMO, the served user has massive and different large-scale fading coefficients to all distributed BS antennas, which leads the corresponding instantaneous channel correlation matrix is modeled as a Gram matrix that each element have different variance. Recently, a toy example 2×2 Gram matrix was investigated in [17], which still had untraceable probability density function (PDF) and its eigenvalues joint PDF was given in integral form, and therefore can be evaluated numerically. In a nutshell, the SE issues in cell-free massive MIMO systems have become exceedingly more challenging and complex.

A. Related Work

In light of this fact, the fields of cell-free massive MIMO still have seen very rapid growth during the last years. A great amount of SE results have been reported in the context of linear processing.

On the one hand, a plethora of in-depth studies have been performed based on the non-orthogonal linear maximum-ratio combining/maximum-ratio transmission (MRC/MRT) processing. Specifically, a considerable portion of the open literature (e.g., [13, 18, 21–23]) adopts the structure that the massive BS antennas are assigned to several distributed access points which have multiple-antenna. In [18], by considering imperfect channel state information (CSI), the authors provided the analytical expressions of the achievable uplink/downlink rate, in a single-cell environment, via the applications of the large dimensional random matrix theory [19] and the worst-case technology [20]. Moreover, in the context of multi-cell case, [21] obtained the closed-form expression of the effective signal to interference plus noise ratio (SINR) and, thereafter, proposed a max-min power control scheme to improve the minimum SE performance. In addition, [22] obtained the asymptotic SINR expression, which was utilized to formalize an optimization problem and pursue the optimal system parameters to improve the system's energy efficiency. Also, on [13], the bound results of the achievable downlink rate and its asymptotic properties were reported and analyzed, respectively. Further, by using downlink training to obtain the estimated effective CSI, the authors in [23] offered and analyzed the approximate achievable downlink rate closed-form expressions, and compared with the perfect effective CSI case. Apart from the above mentioned classic antenna deployment, a critical structure is to randomly place each BS antenna in a given area, which brings about more challenging in performance analysis and is adopted by [12, 24–29]. In the downlink with perfect CSI, [24] showed the exact achievable downlink rate expression which was given in special function form, and analyzed its asymptotic performance by using a complicated upper-bound result. From another angle to easily analyze the rate performance, we first note the fundamental cell-free massive MIMO work of Ngo *et al.* [12] in which smartly proposed the exact, simple, and tractable closed-form expressions of the achievable uplink/downlink rate with imperfect CSI based the methodology of effective SINR, and designed near-optimal power allocation scheme to greatly promote the uplink/downlink minimum rate performance. Hence, triggered by [12], both [25] and [26] considered the max-min SINR optimization problem and came up with the corresponding power allocation methods in the

uplink and downlink, respectively. Moreover, the rate performance issue of downlink multicast was evaluated in [27], and [28] implied that using downlink pilots can effectively improve the system performance. Also, a power control scheme was provided by [29] to reduce the power consumption. Essentially, the issues around the SE based on linear MRC/MRT processing for cell-free massive MIMO systems have been largely and extensively characterized, and its behaviors become more and more clear.

On the other hand, despite the orthogonal linear zero-forcing (ZF) processing can eliminate the multi-user interference effectively, there are relatively few theory results on it for the cell-free massive MIMO systems. With perfect CSI assumption, in [30], the approximate closed-form expression of the achievable uplink rate was obtained in the complicated Laguerre polynomial form based on the Gauss-Laguerre quadrature rule. Also, [31] considered the special case that the BS antennas are distributed uniformly on a ring, and, thereafter, provided the asymptotic achievable uplink rate expression in closed-form result which contained the Legendre function and Gauss hypergeometric function. Moreover, in the downlink, a lower-bound result of the achievable downlink rate was given in integral form and the corresponding asymptotic result showed that it becomes infinite as the number of BS antennas grows unbound [24]. With imperfect CSI assumption, [13] and [23] also provided the corresponding bound results of the achievable downlink rate with ZF precoder, which the corresponding expressions seem untraceable. Moreover, [26] invested the maximizing the minimum downlink SINR optimization problem based on the ZF precoder. However, the corresponding effective SINR is the function of small-scale fading, which the similar case can also be found in [32]. Hence, to the best of the authors' knowledge, little is still known about more computationally and insightful analytical achievable rate results in cell-free massive MIMO systems with linear ZF processing.

B. Our Contribution

Motivated by the previous discussion, in this paper, we are primarily involved in the SE analysis of the ZF detector over the cell-free massive MIMO systems, which this generic framework applies for both perfect CSI and imperfect CSI cases. Primarily, for the perfect CSI case, we study the achievable uplink rate performance and propose the approximate closed-form expressions of its upper-bound and lower-bound, respectively, which depend only on the large-scale fading coefficients and are in a reduced form. Particularly, it is important to note that those obtained bound results can degrade into the corresponding bound results in the conventional massive

MIMO systems, which shows its universality. Further, by averaging out the large-scale fading coefficients, the asymptotic analysis reflect that, as the number of BS antennas L becomes infinite, both obtained upper-bound and lower-bound of the achievable uplink rate have an asymptotic lower-bound $\frac{\alpha}{2} \log_2 L$, which α denotes the path-loss factor that is often larger than 2 except the free space environment. However, for the conventional massive MIMO systems, the bounds has just the asymptotically tight bound $\log_2 L$. It means that the cell-free massive MIMO systems have the better rate performance experience than the conventional massive MIMO systems since it offers extra *distance diversity* thanks to the massively distributed antennas. Secondly, for the imperfect CSI case, the similar bound results and conclusions in perfect CSI case can also be obtained and deduced, respectively, but only with a little bit rate loss. Apart from that, it is found that the obtained bound results in imperfect CSI case degrade into the corresponding bound results in perfect CSI case when the power for using channel estimation is large enough. Finally, the numerical simulation has validated the effectiveness of as mentioned above.

C. Organization and Notation

The rest of the paper is organized as follows. The channel model and uplink data transmission are described in Section II. The analysis of SE with perfect CSI is presented in Section III. The analysis of SE with imperfect CSI is presented in Section IV. Section V provides the simulation results to verify the effectiveness of the obtained results in Section III and Section IV. Finally, conclusion is given in Section VI.

Throughout this paper, lower-case and upper-case boldface letters denote vectors and matrices, respectively. $\mathbb{C}^{M \times K}$ denotes the $M \times K$ complex space. \mathbf{A}^\dagger and \mathbf{A}^{-1} denote the Hermitian transpose and the inverse of the matrix \mathbf{A} , respectively. \mathbf{I}_M denotes an $M \times M$ identity matrix. $\mathbf{0}_{M \times K}$ denotes an $M \times K$ zero matrix. The $\mathbb{E}_X\{\cdot\}$ denotes expectation with respect to the random variable X . A complex Gaussian random vector \mathbf{x} is denoted as $\mathbf{x} \sim \mathcal{CN}(\bar{\mathbf{x}}, \Sigma)$, where the mean vector is $\bar{\mathbf{x}}$ and the covariance matrix is Σ . $\|\cdot\|_2$ denotes the 2-norm of a vector. $\text{diag}(\mathbf{a})$ denotes a diagonal matrix where the main diagonal entries are the elements of vector \mathbf{a} . $\Gamma(x) = \int_0^\infty t^{x-1} e^{-t} dt$ is the Gamma function. Finally, $f(L) = \Theta(g(L))$, $f(L) = O(g(L))$, and $f(L) = \Omega(g(L))$ mean that $g(L)$ is an asymptotically tight bound, an asymptotic upper-bound, and an asymptotic lower-bound for $f(L)$ as $L \rightarrow \infty$, respectively, which the corresponding definitions can be found in [33, Ch. 3.1].

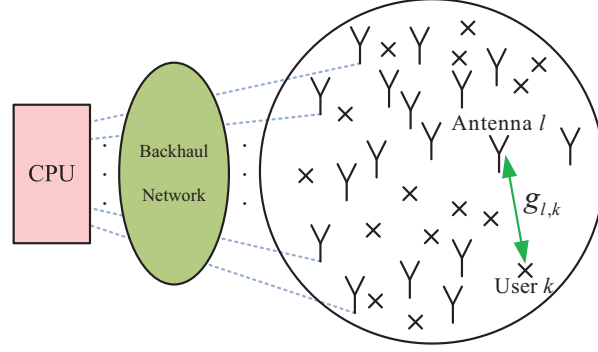


Fig. 1. Schematic illustration of a cell-free massive MIMO system with a circular area. X-shaped and Y-shaped icons denote a user and a BS antenna, respectively.

II. SYSTEM MODEL

We consider a cell-free massive MIMO system. This system has L BS antennas and K ($L \gg K$) single-antenna users, which are uniformly distributed within a circular area. All L BS antennas are linked to an central processing unit (CPU) based on a backhaul network which is used by each BS antenna to perform uploading/downloading network information, i.e., received signal, CSI, and etc. The whole system is demonstrated in Fig. 1. For convenience, we assume that the whole system adopts a time-division duplexing (TDD) protocol, as well as, the BS and all users are perfectly synchronized in each symbol. Without loss of generality, the radius of this circular area is reduced to 1.

A. Channel Model

Let us focus on the channel model. \mathbf{g}_k denotes the $L \times 1$ channel gain vector between the user k and all L BS antennas, which is given by

$$\mathbf{g}_k = \sqrt{\text{diag}(\boldsymbol{\gamma}_k)} \mathbf{h}_k, \quad (1)$$

where $\mathbf{h}_k = [h_{1,k}, \dots, h_{l,k}, \dots, h_{L,k}]^T \sim \mathcal{CN}(\mathbf{0}_{L \times 1}, \mathbf{I}_L)$ denotes the $L \times 1$ small-scale fading vector and $\boldsymbol{\gamma}_k = [\gamma_{1,k}, \dots, \gamma_{l,k}, \dots, \gamma_{L,k}]^T$ denotes the $L \times 1$ large-scale fading vector, which characterizes the long-term channel effect such as path-loss and shadowing. To be more specific, the l th entry of the vector \mathbf{g}_k , $g_{l,k}$, is written as

$$g_{l,k} = h_{l,k} \gamma_{l,k}^{\frac{1}{2}}. \quad (2)$$

Without loss of generality, we ignore the shadowing effect and model the large-scale fading coefficient $\gamma_{l,k}$ as [10, 11, 24]

$$\gamma_{l,k} = d_{l,k}^{-\alpha}, \quad (3)$$

where $d_{l,k}$ is the distance between the l th BS antenna and user k , and $\alpha > 0$ denotes the path-loss factor. Also, as shown in Fig. 1, γ_k has unequal entries since the user k in the circular area has different access distances to all L BS antennas. Here, the block fading assumption [16] is adopted, which means that the large-scale fading coefficients are kept fixed over lots of coherence time intervals and the small-scale fading coefficients remain fixed within a coherence time interval and change between any two adjacent coherence time intervals. Moreover, based on the above mentioned slow-varying characteristic of the large-scale fading which is able to be obtained by channel measurement and feedback [11], we assume that it can be perfectly obtained by the BS side. Also, at the same time, the assumption is taken that each user's channel is independent from other users' channels.

B. Uplink Data Transmission

In case of the uplink data transmission, after all K users send uplink data to the BS synchronously, the received signal vector $\mathbf{y} \in \mathbb{C}^{L \times 1}$ at the BS is modeled as

$$\mathbf{y} = \sqrt{\rho_u} \sum_{k=1}^K \mathbf{g}_k s_k + \mathbf{z} = \sqrt{\rho_u} \mathbf{G} \mathbf{s} + \mathbf{z}, \quad (4)$$

where s_k is the normalized transmitted symbol of user k which is the k th entry of vector $\mathbf{s} \in \mathbb{C}^{K \times 1}$ with the conditions of $\mathbb{E}_{\mathbf{s}}\{\mathbf{s}\} = \mathbf{0}_{K \times 1}$ and $\mathbb{E}_{\mathbf{s}}\{\mathbf{s}\mathbf{s}^\dagger\} = \mathbf{I}_K$, ρ_u denotes the average uplink symbol power of each user, and $\mathbf{z} \sim \mathcal{CN}(\mathbf{0}_{L \times 1}, \mathbf{I}_L)$ denotes the received noise vector at the BS in cell j . Also, $\mathbf{G} = [\mathbf{g}_1, \dots, \mathbf{g}_k, \dots, \mathbf{g}_K] \in \mathbb{C}^{L \times K}$ is the channel matrix between all users and the BS antennas. It is important to note that, in the following, the achievable rate analysis for both perfect CSI and imperfect CSI assumptions relies on (4) heavily.

III. SE ANALYSIS WITH PERFECT CSI

In this section, we introduce the achievable uplink rate model with perfect CSI assumption, obtain its approximate closed-form upper-bound and lower-bound expressions and, thereafter, aim to analyze its asymptotic performance.

A. Achievable Uplink Rate Model

We firstly investigate the case that the BS knows the total channel gain, i.e., \mathbf{G} . Hence, the received signal \mathbf{y} in (4) is separated into K streams by multiplying it with the linear detector matrix $\mathbf{A} \in \mathbb{C}^{L \times K}$ which is constituted by \mathbf{G} . The processed signal is given by

$$\mathbf{r} = \mathbf{A}^\dagger \mathbf{y} \in \mathbb{C}^{K \times 1}. \quad (5)$$

Then, the k th entry of \mathbf{r} , r_k , is modeled as

$$r_k = \sqrt{\rho_u} \mathbf{a}_k^\dagger \mathbf{g}_k s_k + \sqrt{\rho_u} \sum_{n \neq k}^K \mathbf{a}_k^\dagger \mathbf{g}_n s_n + \mathbf{a}_k^\dagger \mathbf{z}, \quad (6)$$

where \mathbf{a}_k is the k th column of \mathbf{A} . Note that the desire signal of user k is $\sqrt{\rho_u} \mathbf{a}_k^\dagger \mathbf{g}_k s_k$ while the rest of in (6) is regarded as the interference signal. By modeling the interference signal as an Gaussian noise, utilizing the worst case technology in [20, Theorem 1], adopting the standard linear ZF detector $\mathbf{A} = \mathbf{G} (\mathbf{G}^\dagger \mathbf{G})^{-1}$, and normalizing the total system bandwidth into unity, hence the SE of user k is the achievable uplink rate over a lot of realizations of the small-scale fading part in \mathbf{G} , in units of Bits/Hz/sec, which is given by [16, Eq. (18)]

$$R_k = \mathbb{E}_{\mathbf{H}} \left\{ \log_2 \left(1 + \frac{\rho_u}{\|\mathbf{a}_k\|_2^2} \right) \right\}, \quad (7)$$

where

$$\mathbf{H} \triangleq [\mathbf{h}_1, \dots, \mathbf{h}_k, \dots, \mathbf{h}_K] \in \mathbb{C}^{L \times K}. \quad (8)$$

It is important to note that (7) depends on the antenna topology of all L BS antennas that different antenna topology means different R_k . Hence, it is necessary to evaluate the achievable uplink rate by averaging out the antenna topology or large-scale fading. We also defining the following rate metric

$$\bar{R}_k = \mathbb{E}_{\mathbf{\Upsilon}} \{R_k\}, \quad (9)$$

where

$$\mathbf{\Upsilon} \triangleq [\gamma_1, \dots, \gamma_k, \dots, \gamma_K] \in \mathbb{C}^{L \times K}. \quad (10)$$

B. Upper-Bound

The following key theorem presents an approximate closed-form expression for the upper-bound of the user k 's achievable uplink rate R_k . To the best of our knowledge, this result is also new.

Theorem 1: An upper-bound of R_k , R_k^{ub} , has an approximate closed-form expression when L is large, which is given by

$$R_k^{\text{ub}} \approx \widetilde{R_k^{\text{ub}}} \triangleq \log_2 \left(1 + \rho_u \sum_{\tilde{l} \in \mathcal{L}_k} \gamma_{\tilde{l},k} \right), \quad (11)$$

where $\mathcal{L}_k = \mathcal{L}/\mathcal{A}_k$ and $\mathcal{L} = \{l | \forall l = 1, \dots, L\}$. Also, \mathcal{A}_k is defined as

$$\mathcal{A}_k \triangleq \text{Unique} \left(\left\{ l_n^* = \arg \max_l \gamma_{l,n} \mid \forall n \neq k \right\} \right), \quad (12)$$

and $\text{Unique}(\mathcal{T})$ returns the same values as in set \mathcal{T} but with no repetitions.

Proof: Based on the Jensen's inequality [16], (7) is upper-bounded by

$$R_k \leq \log_2 \left(1 + \rho_u \mathbb{E}_{\mathbf{H}} \left\{ \frac{1}{\|\mathbf{a}_k\|_2^2} \right\} \right) \triangleq R_k^{\text{ub}}, \quad (13)$$

where the “=” in “ \leq ” is reached when $\frac{1}{\|\mathbf{a}_k\|_2^2}$ is a constant. Hence, the key issue is to obtain the distribution of $\frac{1}{\|\mathbf{a}_k\|_2^2}$. Based on the results in [19, Theorem A.4] and [24, Eq. (62)], when L is large, $\frac{1}{\|\mathbf{a}_k\|_2^2}$ is approximated by

$$\frac{1}{\|\mathbf{a}_k\|_2^2} \approx \|\mathbf{g}_k\|_2^2 - \sum_{n \neq k}^K |g_{l_n^*,k}|^2, \quad (14)$$

where l_n^* is defined as in (12). With large L , for $\forall n_1, n_2$ ($n_1 \neq n_2$), the probability of the two users n_1 and n_2 are close to the same BS antenna is very low, i.e., $\Pr \{l_{n_1}^* = l_{n_2}^* | n_1 \neq n_2\} \rightarrow 0$. Hence, we have

$$\sum_{n \neq k}^K |g_{l_n^*,k}|^2 \approx \sum_{\tilde{l} \in \mathcal{A}_k} |g_{\tilde{l},k}|^2. \quad (15)$$

Finally, (11) is obtained by substituting (2), (14), and (15) into (13) and simplifying. \blacksquare

It is important to note that the result in *Theorem 1* does not depend on the small-scale fading and is constituted by a series of large-scale fading coefficients. Also, based on (11) and the special structure of (12), it is found that, for the approximate upper-bound of R_k , at most $K - 1 \geq |\mathcal{A}_k|$ large-scale coefficients become useless after the BS processes the received signal vector \mathbf{y} in (4) by the ZF detector. Intuitively, the essence of the user k 's detector \mathbf{a}_k is to project the signal vector

\mathbf{g}_k onto the nullspace of the interference space spanned by $\{\mathbf{g}_n | \forall n \neq k\}$. Since the direction of \mathbf{g}_n is mostly decided by its l_n^* th component $g_{l_n^*, n}$, the approximation (14) holds; in other words, the l_n^* th component of \mathbf{g}_k , $g_{l_n^*, k}$, is eliminated. In a nutshell, from both theorem analysis and physics intuition perspectives, the obtained approximate upper-bound of R_k in *Theorem 1* not only has its rationality, but also this closed-form expression allows us to pursue the benefit of the important system design. In spite of the large L assumption in *Theorem 1*, it is worth mentioning that the corresponding result is still valid with a not-so-large number of antennas in section V. To gain more insights, when $L \rightarrow \infty$, $|\mathcal{L}_k| \rightarrow L - K + 1$ and then to consider the case of $\forall l, \gamma_{l,k} = \gamma_k$ or to place all the BS antennas together, hence $\widetilde{R}_k^{\text{ub}}$, after much algebraic manipulation, becomes

$$\widetilde{R}_k^{\text{ub}} \rightarrow \log_2 (1 + \rho_u (L - K + 1) \gamma_k). \quad (16)$$

Note that (16) is the exact upper-bound of the achievable uplink rate with ZF detector and perfect CSI in a conventional massive multiple-input multiple-output (MIMO) system given by [34, Theorem 3] if the corresponding inter-cell interference is ignored. In a nutshell, *Theorem 1* provides a very generic upper-bound expression (11) to approximate the limit system performance.

Also, it is important to note that different large-scale fading makes different (11). The following corollary will be used for investigating the asymptotic performance of the approximate upper-bound of R_k by averaging out the large-scale fading.

Corollary 1: An upper-bound of \bar{R}_k , \bar{R}_k^{ub} , has the following approximation

$$\bar{R}_k^{\text{ub}} \approx \widetilde{\bar{R}_k^{\text{ub}}} \triangleq \mathbb{E}_{\mathbf{r}} \left\{ \widetilde{R}_k^{\text{ub}} \right\}. \quad (17)$$

Also, when $L \rightarrow \infty$, $\widetilde{\bar{R}_k^{\text{ub}}} = \Omega(\frac{\alpha}{2} \log_2 L)$.

Proof: Based on *Theorem 1*, it is easy to obtain the approximation (17). In the following, the asymptotic behaviour of $\widetilde{\bar{R}_k^{\text{ub}}}$ is proved.

First, by denoting $\gamma_k^{(l)}$ and $d_k^{(l)}$ as the l th maximum large-scale fading coefficient and the l th minimum access distance from user k to the antennas belonged to the set \mathcal{L}_k , respectively, $\widetilde{\bar{R}_k^{\text{ub}}}$ is rewritten and lower-bounded by

$$\widetilde{\bar{R}_k^{\text{ub}}} = \mathbb{E}_{\mathbf{r}} \left\{ \log_2 \left(1 + \rho_u \sum_{l=1}^{|\mathcal{L}_k|} \gamma_k^{(l)} \right) \right\} > \mathbb{E}_{\mathbf{r}} \left\{ \log_2 \left(1 + \rho_u \gamma_k^{(1)} \right) \right\} \triangleq \widetilde{\bar{R}_k^{\text{ub-lb}}}. \quad (18)$$

Then, when L is large, $|\mathcal{L}_k| \rightarrow L - K + 1$ and \mathcal{L}_k can be regarded and composed of $L - K + 1$ uniformly distributed BS antennas in the circular area with unit radius [24]. Hence, with the aid of (3) and the Jensen's inequality, $\widetilde{R}_k^{\text{ub-lb}}$ is rewritten and lower-bounded by

$$\widetilde{R}_k^{\text{ub-lb}} = \int_0^1 f_{\rho_k}(x) dx \int_0^{1+x} f_{d_k^{(1)}|\rho_k}(y|x) \log_2(1 + \rho_u y^{-\alpha}) dy \geq \log_2\left(1 + \frac{\rho_u}{Q_1(L)}\right), \quad (19)$$

where the “=” in “ \geq ” is reached when $d_k^{(1)}$ is a constant. $f_{\rho_k}(x)$ and $f_{d_k^{(1)}|\rho_k}(y|x)$ are the PDF of ρ_k (The distance between user k and the circular area centre) and the conditional PDF of $d_k^{(1)}$ given ρ_k , which the corresponding detail expressions can be found in (69) and (70), respectively, in the *Lemma 1* of Appendix A. Also, $Q_1(L)$ is the special case of (74) in the *Proposition 1* of Appendix A, which has the property $Q_1(L) = \Theta(L^{-\frac{\alpha}{2}})$.

Finally, this asymptotic conclusion is obtained based on the relationship among $Q_1(L)$, (18), and (19). ■

It is interesting to note from *Corollary 1* that the asymptotic behaviour of the approximate upper-bound of \bar{R}_k shows that the corresponding growth rate of the approximate upper-bound achievable uplink rate, by averaging out both the small-scale fading and large-scale fading, is not only the logarithmic function of the number of BS antennas L but also the linear function of the path-loss factor α . The underlying reason behind this phenomenon is that the different access distances from the user to the massive distributed BS antennas offer extra *distance diversity* compared with the case when all massive BS antennas are placed together. So far as is known to the authors, the results as in *Corollary 1* have not been disseminated in the open literature before.

C. Lower-Bound

We now focus on the case of the lower-bound analysis of the achievable uplink rate R_k . The following theorem establishes a new approximate lower-bound, which applies for arbitrary number of BS antennas and arbitrary uplink data power.

Theorem 2: A lower-bound of R_k , R_k^{lb} , has an approximate closed-form expression when L is large, which is given by

$$R_k^{\text{lb}} \approx \widetilde{R}_k^{\text{lb}} \triangleq \log_2(1 + \rho_u \Phi_k(\Psi_k - 1)), \quad (20)$$

where Φ_k and Ψ_k are defined as

$$\Phi_k \triangleq \frac{\sum_{\tilde{l} \in \mathcal{L}_k} \gamma_{\tilde{l},k}^2}{\sum_{\tilde{l} \in \mathcal{L}_k} \gamma_{\tilde{l},k}}, \quad (21)$$

$$\Psi_k \triangleq \frac{\left(\sum_{\tilde{l} \in \mathcal{L}_k} \gamma_{\tilde{l},k} \right)^2}{\sum_{\tilde{l} \in \mathcal{L}_k} \gamma_{\tilde{l},k}^2}, \quad (22)$$

respectively.

Proof: Based on the Jensen's inequality, (7) is lower-bounded by

$$R_k \geq \log_2 \left(1 + \frac{\rho_u}{\mathbb{E}_{\mathbf{H}} \{ \|\mathbf{a}_k\|_2^2 \}} \right) \triangleq R_k^{\text{lb}}, \quad (23)$$

where the “=” in “ \geq ” is reached when $\|\mathbf{a}_k\|_2^2$ is a constant. Hence, the key issue is to obtain the distribution of $\|\mathbf{a}_k\|_2^2$. By substituting (14) and (15) into it, $\|\mathbf{a}_k\|_2^2$ is approximated by

$$\|\mathbf{a}_k\|_2^2 \approx \frac{1}{\sum_{\tilde{l} \in \mathcal{L}_k} |g_{\tilde{l},k}|^2}. \quad (24)$$

Based on (2), it is note that $\forall \tilde{l} \in \mathcal{L}_k$, $|g_{\tilde{l},k}|^2 \sim \Gamma(1, \gamma_{\tilde{l},k})$ which the Gamma distributed random variable $x \sim \Gamma(\eta, \theta)$ has the PDF $f(x) = \frac{x^{\eta-1} e^{-\frac{x}{\theta}}}{\theta^\eta \Gamma(\eta)}$, $x \geq 0$. Then, via the application of *Lemma 2* in Appendix A, $\sum_{\tilde{l} \in \mathcal{L}_k} |g_{\tilde{l},k}|^2$ can be approximated by the Gamma distributed random variable $\Lambda_k \sim \Gamma(\Psi_k, \Phi_k)$. Hence, based on the above mentioned results, after some algebraic manipulation, we perform the following sequence of operations

$$\mathbb{E}_{\mathbf{H}} \{ \|\mathbf{a}_k\|_2^2 \} \approx \mathbb{E}_{\Lambda_k} \left\{ \frac{1}{\Lambda_k} \right\} = \frac{1}{\Phi_k (\Psi_k - 1)}. \quad (25)$$

Finally, (20) is obtained by substituting (25) into (23). ■

It is important to note that, to our knowledge, the result in *Theorem 2* presents the first simple analytical investigation of the lower-bound of the achievable uplink rate R_k for the case of each BS antennas is uniformly distributed. It is also worth noting that, as $L \rightarrow \infty$, by taking the same assumption for obtaining (16), hence $\widetilde{R}_k^{\text{lb}}$, after much algebraic manipulation, becomes

$$\widetilde{R}_k^{\text{lb}} \rightarrow \log_2 (1 + \rho_u (L - K) \gamma_k). \quad (26)$$

It is well known that (26) is the exact lower-bound of the achievable uplink rate with ZF detector and perfect CSI in a conventional massive MIMO system given by [16, Proposition 3]. Based on this fact, *Theorem 2* provides an useful lower-bound formula to assess the achievable uplink rate

performance for the general communication system. Moreover, it is obvious that $\widetilde{R}_k^{\text{lb}}$ is always smaller than $\widetilde{R}_k^{\text{ub}}$, which implies the validity of *Theorem 2*. Next, it is interesting to consider the scaling behavior of the obtained approximate lower-bound by averaging out the large-scale fading.

Corollary 2: An lower-bound of \bar{R}_k , \bar{R}_k^{lb} , has the following approximation

$$\bar{R}_k^{\text{lb}} \approx \widetilde{\bar{R}}_k^{\text{lb}} \triangleq \mathbb{E}_{\mathbf{r}} \left\{ \widetilde{R}_k^{\text{lb}} \right\}. \quad (27)$$

Also, when $L \rightarrow \infty$, $\widetilde{\bar{R}}_k^{\text{lb}} = \Omega(\frac{\alpha}{2} \log_2 L)$.

Proof: Based on *Theorem 2*, it is easy to obtain the approximation (27). In the following, the asymptotic behaviour of $\widetilde{\bar{R}}_k^{\text{lb}}$ is proved.

First, by adopting the similar sorting method of large-scale fading coefficient as in *Corollary 1*, $\widetilde{R}_k^{\text{lb}}$ is rewritten as

$$\widetilde{R}_k^{\text{lb}} = \mathcal{F} \left(\gamma_k^{(1)}, \gamma_k^{(2)}, \dots, \gamma_k^{(|\mathcal{L}_k|-1)}, \gamma_k^{(|\mathcal{L}_k|)} \right) = \log_2 (1 + \rho_u \Phi_k^{\text{sort}} (\Psi_k^{\text{sort}} - 1)), \quad (28)$$

where Φ_k^{sort} and Ψ_k^{sort} are defined as

$$\Phi_k^{\text{sort}} \triangleq \frac{\sum_{l=1}^{|\mathcal{L}_k|} \left(\gamma_k^{(l)} \right)^2}{\sum_{l=1}^{|\mathcal{L}_k|} \gamma_k^{(l)}}, \quad (29)$$

$$\Psi_k^{\text{sort}} \triangleq \frac{\left(\sum_{l=1}^{|\mathcal{L}_k|} \gamma_k^{(l)} \right)^2}{\sum_{l=1}^{|\mathcal{L}_k|} \left(\gamma_k^{(l)} \right)^2}, \quad (30)$$

respectively. Then, $\forall t = 1, \dots, |\mathcal{L}_k|$, it is obvious that

$$\frac{\partial \widetilde{R}_k^{\text{lb}}}{\partial \gamma_k^{(t)}} = \frac{\sum_{l \neq t}^{|\mathcal{L}_k|} \gamma_k^{(l)} + \left(\sum_{l \neq t}^{|\mathcal{L}_k|} \gamma_k^{(l)} \right)^2}{\Phi_k^{\text{sort}} (\Psi_k^{\text{sort}} - 1) \left(\sum_{l=1}^{|\mathcal{L}_k|} \gamma_k^{(l)} \right)^2} \log_2 e > 0. \quad (31)$$

By substituting (28) into $\widetilde{\bar{R}}_k^{\text{lb}}$ and unitizing (31), we get

$$\widetilde{\bar{R}}_k^{\text{lb}} > \mathbb{E}_{\mathbf{r}} \left\{ \mathcal{F} \left(\gamma_k^{(2)}, \gamma_k^{(2)}, \dots, 0, 0 \right) \right\} = \mathbb{E}_{\mathbf{r}} \left\{ \log_2 \left(1 + \rho_u \gamma_k^{(2)} \right) \right\} \triangleq \widetilde{\bar{R}}_k^{\text{lb-lb}}. \quad (32)$$

Next, utilizing (3) and the methodology of (19), after some manipulations, $\widetilde{\bar{R}}_k^{\text{lb-lb}}$ is lower-bounded by

$$\widetilde{\bar{R}}_k^{\text{lb-lb}} = \int_0^1 f_{\rho_k}(x) dx \int_0^{1+x} f_{d_k^{(2)}|\rho_k}(y|x) \log_2(1 + \rho_u y^{-\alpha}) dy \geq \log_2\left(1 + \frac{\rho_u}{Q_2(L)}\right), \quad (33)$$

where the “=” in “ \geq ” is reached when $d_k^{(2)}$ is a constant, $f_{d_k^{(2)}|\rho_k}(y|x)$ is the conditional PDF of $d_k^{(2)}$ given ρ_k which is the special case of (70) in the *Lemma 1* of Appendix A, and $Q_2(L) = \Theta(L^{-\frac{\alpha}{2}})$ is the special case of (74) in the *Proposition 1* of Appendix A.

Finally, the corresponding asymptotic performance of *Corollary 2* can be obtained by the above mentioned results. ■

It is important to note that an analogous result has also been derived in *Corollary 1*. To gain more sights, the conclusions in *Corollary 1* and *Corollary 2* implies that the obtained approximate upper-bound and lower-bound, which line at either end of the achievable uplink rate with perfect CSI, has the same asymptotic lower-bound $\frac{\alpha}{2} \log_2 L$ and the path-loss factor α is always larger than 2 unless in the case of free space propagation. Interestingly, by placing all antennas at the area centre and averaging out the large-scale fading, based on (16) and (26), it is found that the achievable uplink rate of ZF detector with perfect CSI in the conventional massive MIMO system is just $\Theta(\log_2 L)$ which its growth rate is no further than $\log_2 L$. In brief, cell-free massive MIMO systems promise better achievable uplink rate performance than the conventional massive MIMO systems based on the conditions of the perfect CSI assumption and ZF detector. In the following section, the in-depth studies have been made on the achievable uplink rate analysis with imperfect CSI case.

IV. SE ANALYSIS WITH IMPERFECT CSI

In this section, we introduce the achievable uplink rate model with imperfect CSI assumption, obtain its approximate closed-form upper-bound and lower-bound expressions and, thereafter, aim to analyze its asymptotic performance.

A. Achievable Uplink Rate Model

In real communication system, a key component is to obtain the CSI between the users and the BS antennas. In TDD model, all users firstly send uplink pilot sequence to the BS which knows the exact pilot sequence information. Then, the BS utilizes these pilot sequences and the statistical information to estimate all users' channels. When the typical minimum mean squared

error estimation method [35] and the orthogonal pilot sequences [5, 16] are adopted, the total channel \mathbf{G} is estimated as

$$\hat{\mathbf{G}} \triangleq [\hat{\mathbf{g}}_1, \dots, \hat{\mathbf{g}}_k, \dots, \hat{\mathbf{g}}_K] \in \mathbb{C}^{L \times K}, \quad (34)$$

where $\hat{\mathbf{g}}_k = [\hat{g}_{1,k}, \dots, \hat{g}_{L,k}]^T \in \mathbb{C}^{L \times 1}$ is the estimated channel vector of \mathbf{g}_k . Also, $\forall k$, $\tilde{\mathbf{g}}_k$ and the corresponding estimate error vector $\tilde{\mathbf{g}}_k \triangleq \mathbf{g}_k - \hat{\mathbf{g}}_k$ follow

$$\hat{\mathbf{g}}_k \sim \mathcal{CN}(\mathbf{0}_{L \times 1}, \text{diag}(\hat{\gamma}_{1,k}, \dots, \hat{\gamma}_{L,k})), \quad (35)$$

$$\tilde{\mathbf{g}}_k \sim \mathcal{CN}(\mathbf{0}_{L \times 1}, \text{diag}(\tilde{\gamma}_{1,k}, \dots, \tilde{\gamma}_{L,k})), \quad (36)$$

and satisfy $\mathbb{E}_{\mathbf{h}_k} \{\hat{\mathbf{g}}_k^\dagger \tilde{\mathbf{g}}_k\} = 0$, where

$$\hat{\gamma}_{l,k} \triangleq \frac{\rho_p \gamma_{l,k}}{\rho_p \gamma_{l,k} + 1} \gamma_{l,k}, \quad (37)$$

$$\tilde{\gamma}_{l,k} \triangleq \frac{1}{\rho_p \gamma_{l,k} + 1} \gamma_{l,k}, \quad (38)$$

and ρ_p denotes the pilot sequence power. Similar as the perfect CSI case, we multiply (4) with the linear detector $\hat{\mathbf{A}}$ constituted by $\hat{\mathbf{G}}$ as follow

$$\hat{\mathbf{r}} = \hat{\mathbf{A}}^\dagger \mathbf{y}. \quad (39)$$

Then, the k th entry of $\hat{\mathbf{r}}$, \hat{r}_k , is given by

$$\hat{r}_k = \sqrt{\rho_u} \hat{\mathbf{a}}_k^\dagger \mathbf{g}_k s_k + \sqrt{\rho_u} \sum_{n \neq k}^K \hat{\mathbf{a}}_k^\dagger \mathbf{g}_n s_n + \hat{\mathbf{a}}_k^\dagger \mathbf{z}, \quad (40)$$

where $\hat{\mathbf{a}}_k$ is the k th column of $\hat{\mathbf{A}}$. Since the BS estimates \mathbf{G} as $\hat{\mathbf{G}}$, \hat{r}_k is rewritten as

$$\hat{r}_k = \sqrt{\rho_u} \hat{\mathbf{a}}_k^\dagger \hat{\mathbf{g}}_k s_k + \sqrt{\rho_u} \sum_{n \neq k}^K \hat{\mathbf{a}}_k^\dagger \hat{\mathbf{g}}_n s_n + \sqrt{\rho_u} \sum_{n=1}^K \hat{\mathbf{a}}_k^\dagger \tilde{\mathbf{g}}_n s_n + \hat{\mathbf{a}}_k^\dagger \mathbf{z}. \quad (41)$$

By adopting the standard ZF detector $\hat{\mathbf{A}} = \hat{\mathbf{G}} \left(\hat{\mathbf{G}}^\dagger \hat{\mathbf{G}} \right)^{-1}$ and using the similar way as in the imperfect CSI case in [16, Eq. (36) & Eq. (41)], after much algebraic manipulation, the achievable uplink rate of the k th user by averaging out the small-scale fading \mathbf{H} is given as

$$\hat{R}_k = \mathbb{E}_{\mathbf{H}} \left\{ \log_2 \left(1 + \frac{\rho_u}{\rho_u \sum_{l=1}^L |\hat{a}_{l,k}|^2 \sum_{n=1}^K \tilde{\gamma}_{l,n} + \|\hat{\mathbf{a}}_k\|_2^2} \right) \right\}, \quad (42)$$

where $\hat{a}_{l,k}$ is the l th entry of $\hat{\mathbf{a}}_k$. Note that with high ρ_p , i.e., $\tilde{\gamma}_{l,n} \rightarrow 0, \forall l, n$, and $\hat{\mathbf{a}}_k \rightarrow \mathbf{a}_k$, \hat{R}_k becomes the perfect CSI case as in (7).¹ Moreover, by following the methodology in the perfect CSI case, the achievable uplink rate of the k th user by averaging out both small-scale fading and large-scale fading is given by

$$\bar{\hat{R}}_k = \mathbb{E}_{\mathbf{r}} \left\{ \hat{R}_k \right\}. \quad (43)$$

B. Upper-Bound

The following theorem presents a closed-form expression for the approximate upper-bound of the user k 's achievable uplink rate \hat{R}_k in the high L regime. This result is similar to the perfect CSI case given in *Theorem 1*, as it does not involve any integral terms. This constitutes a key contribution of this paper.

Theorem 3: An upper-bound of \hat{R}_k , \hat{R}_k^{ub} , has an approximate closed-form expression when L is large, which is given by

$$\hat{R}_k^{\text{ub}} \approx \widetilde{\hat{R}_k^{\text{ub}}} \triangleq \log_2 \left(1 + \frac{\rho_u}{\rho_u \tilde{\gamma}_{\min} + 1} \sum_{\tilde{l} \in \mathcal{L}_k} \hat{\gamma}_{\tilde{l},k} \right), \quad (44)$$

where $\tilde{\gamma}_{\min}$ is defined as

$$\tilde{\gamma}_{\min} \triangleq \min_l \sum_{n=1}^K \tilde{\gamma}_{l,n}. \quad (45)$$

Proof: Based on the Jensen's inequality and the definition of (45), (42) is upper-bounded by

$$\hat{R}_k \leq \log_2 \left(1 + \frac{\rho_u}{\rho_u \tilde{\gamma}_{\min} + 1} \mathbb{E}_{\mathbf{H}} \left\{ \frac{1}{\|\hat{\mathbf{a}}_k\|_2^2} \right\} \right) \triangleq \hat{R}_k^{\text{ub}}, \quad (46)$$

where the “=” in “ \leq ” is reached when both $\frac{1}{\|\hat{\mathbf{a}}_k\|_2^2}$ is a constant and $\sum_{n=1}^K \tilde{\gamma}_{l_1,n} = \sum_{n=1}^K \tilde{\gamma}_{l_2,n}, \forall l_1 \neq l_2$. The following key issue is to obtain the distribution of $\frac{1}{\|\hat{\mathbf{a}}_k\|_2^2}$. Next, based on the results in *Theorem 1*, the relationship between the large-scale fading coefficients $\hat{\gamma}_{l,n}$ and $\gamma_{l,n}$ in (37), and the one-to-one mapping theorem, then, clearly

$$\frac{1}{\|\hat{\mathbf{a}}_k\|_2^2} \approx \sum_{\tilde{l} \in \mathcal{L}_k} |\hat{g}_{\tilde{l},k}|^2. \quad (47)$$

Finally, (44) is obtained by substituting (35) and (47) into (46) and simplifying. ■

¹For the sake of characterizing the variation of the achievable uplink rate from the imperfect CSI case to the perfect CSI case, the channel estimation overhead in the coherence time interval does not take into account as in [16].

Note that the approximate upper-bound expression in *Theorem 3* can be easily evaluated since it primarily involves simple large-scale fading coefficients, uplink data power, and a minimum value which depends on the variance of the channel estimation error, as well as, the standard logarithmic function base 2. Moreover, based on (37), (38), and the structure of $\widetilde{\hat{R}_k^{\text{ub}}}$ in (44), it is obvious that $\widetilde{\hat{R}_k^{\text{ub}}}$ is always smaller than the perfect CSI case $\widetilde{R_k^{\text{ub}}}$ in (11) and satisfies

$$\lim_{\rho_p \rightarrow \infty} \widetilde{\hat{R}_k^{\text{ub}}} = \widetilde{R_k^{\text{ub}}}. \quad (48)$$

Hence, we note that the conclusion of *Theorem 3* gives a universal formula for the approximate upper-bound of achievable uplink rate. Moreover, as $L \rightarrow \infty$, by utilizing the methodology of obtaining (16), hence $\widetilde{\hat{R}_k^{\text{ub}}}$, after much algebraic manipulation, becomes

$$\widetilde{\hat{R}_k^{\text{ub}}} \rightarrow \log_2 \left(1 + \frac{\rho_u (L - K + 1)}{\rho_u \sum_{n=1}^K \frac{\gamma_n}{\rho_p \gamma_n + 1} + 1} \times \frac{\rho_p \gamma_k}{\rho_p \gamma_k + 1} \gamma_k \right). \quad (49)$$

An interesting phenomenon is found that (49) is the exact upper-bound of the achievable uplink rate with ZF detector and imperfect CSI in a conventional massive MIMO system given by the k th component in [36, Theorem 1] when the out-of-cell interference is not considered. Hence, (49) is a special case of (44) if the event of all the BS antennas locate at the same position.

Since the above mentioned results of the approximate upper-bound of the achievable uplink rate \hat{R}_k mainly depends on the antenna topology, the following corollary presents very simple high L regime's asymptotic performance of the approximate upper-bound of \hat{R}_k by averaging out both the large-scale fading and small-scale fading.

Corollary 3: An upper-bound of \hat{R}_k , \bar{R}_k^{ub} , has the following approximation

$$\bar{R}_k^{\text{ub}} \approx \widetilde{\bar{R}_k^{\text{ub}}} \triangleq \mathbb{E}_{\mathbf{r}} \left\{ \widetilde{\hat{R}_k^{\text{ub}}} \right\}. \quad (50)$$

Also, when $L \rightarrow \infty$, $\widetilde{\bar{R}_k^{\text{ub}}} = \Omega(\frac{\alpha}{2} \log_2 L)$.

Proof: Based on *Theorem 3*, it is easy to obtain the approximation (50). In the following, the asymptotic behaviour of $\widetilde{\bar{R}_k^{\text{ub}}}$ is proved.

First, based on (3), (38), and (45), we have the following inequality

$$\tilde{\gamma}_{\min} \leq \frac{K}{\rho_p}, \quad (51)$$

where the “=” in “ \leq ” is reached when all K users and all L antennas are at the same position of the circular area.

Then, by adopting the similar sorting method of large-scale fading coefficient as in *Corollary 1* and substituting (51) into $\widetilde{\hat{R}}_k^{\text{ub}}$, $\widetilde{\hat{R}}_k^{\text{ub}}$ is rewritten and lower-bounded by

$$\widetilde{\hat{R}}_k^{\text{ub}} = \mathbb{E}_{\mathbf{r}} \left\{ \log_2 \left(1 + \frac{\rho_u}{\rho_u \hat{\gamma}_{\min} + 1} \sum_{l=1}^{|\mathcal{L}_k|} \hat{\gamma}_k^{(l)} \right) \right\} > \mathbb{E}_{\mathbf{r}} \left\{ \log_2 \left(1 + \frac{\rho_u}{\rho_u \frac{K}{\rho_p} + 1} \hat{\gamma}_k^{(1)} \right) \right\} \triangleq \widetilde{\hat{R}}_k^{\text{ub-lb}}. \quad (52)$$

Via application of (37), it can be shown that

$$\hat{\gamma}_k^{(1)} \geq \frac{\rho_p 2^{-\alpha}}{\rho_p 2^{-\alpha} + 1} \gamma_k^{(1)}. \quad (53)$$

where the “=” in “ \geq ” is reached when user k is at a boundary point of the circular area, as well as, the BS antennas belonged to \mathcal{L}_k are also at other same boundary point of the circular area, which the line between these two boundary points is through the circular area centre.

Next, utilizing (3) and the methodology of (19), as well as, substituting (53) into (52), after some manipulations, we have

$$\widetilde{\hat{R}}_k^{\text{ub-lb}} \geq \log_2 \left(1 + \frac{\rho_u \rho_p 2^{-\alpha}}{\left(\rho_u \frac{K}{\rho_p} + 1 \right) (\rho_p 2^{-\alpha} + 1) Q_1(L)} \right), \quad (54)$$

where the condition for reaching the “=” in “ \geq ” is the same as (19).

Finally, based on $Q_1(L) = \Theta(L^{-\frac{\alpha}{2}})$ in *Proposition 1* of Appendix A, (52), and (54), the asymptotic conclusion is obtained. ■

Together with *Corollary 1*, *Corollary 3* indicates that if the uplink data power ρ_u , the number of users K , and the path-loss factor α are kept fixed, as well as, the number of BS antennas L is increased, then, different pilot sequence power ρ_p has no effect on the scaling behaviour of the approximate upper bound of \hat{R}_k and is the same as the perfect CSI case.

C. Lower-Bound

The following theorem provides an approximate closed-form expression of the lower-bound of the achievable uplink rate \hat{R}_k , which is a little more complex compared with the perfect CSI case. This result will play a key role in this paper.

Theorem 4: A lower-bound of \hat{R}_k , \hat{R}_k^{lb} , has an approximate closed-form expression when L is large, which is given by

$$\hat{R}_k^{\text{lb}} \approx \widetilde{\hat{R}}_k^{\text{lb}} \triangleq \log_2 \left(1 + \frac{\rho_u}{\rho_u \hat{\gamma}_{\max} + 1} \hat{\Phi}_k \left(\hat{\Psi}_k - 1 \right) \right), \quad (55)$$

where $\tilde{\gamma}_{\max}$, $\hat{\Phi}_k$, and $\hat{\Psi}_k$ are defined as

$$\tilde{\gamma}_{\max} \triangleq \max_l \sum_{n=1}^K \tilde{\gamma}_{l,n}, \quad (56)$$

$$\hat{\Phi}_k \triangleq \frac{\sum_{\tilde{l} \in \mathcal{L}_k} \hat{\gamma}_{\tilde{l},k}^2}{\sum_{\tilde{l} \in \mathcal{L}_k} \hat{\gamma}_{\tilde{l},k}}, \quad (57)$$

$$\hat{\Psi}_k \triangleq \frac{\left(\sum_{\tilde{l} \in \mathcal{L}_k} \hat{\gamma}_{\tilde{l},k} \right)^2}{\sum_{\tilde{l} \in \mathcal{L}_k} \hat{\gamma}_{\tilde{l},k}^2}, \quad (58)$$

respectively.

Proof: Based on the Jensen's inequality and the definition of (56), (42) is lower-bounded by

$$\hat{R}_k \geq \log_2 \left(1 + \frac{\rho_u}{(\rho_u \tilde{\gamma}_{\max} + 1) \mathbb{E}_{\mathbf{H}} \{ \|\hat{\mathbf{a}}_k\|_2^2 \}} \right) \triangleq \hat{R}_k^{\text{lb}}, \quad (59)$$

where the “=” in “ \geq ” is reached when both $\|\hat{\mathbf{a}}_k\|_2^2$ is a constant and $\sum_{n=1}^K \tilde{\gamma}_{l_1,n} = \sum_{n=1}^K \tilde{\gamma}_{l_2,n}, \forall l_1 \neq l_2$. The following key issue is to obtain the distribution of $\|\hat{\mathbf{a}}_k\|_2^2$. By substituting (47) into it, $\|\hat{\mathbf{a}}_k\|_2^2$ is approximated by

$$\|\hat{\mathbf{a}}_k\|_2^2 \approx \frac{1}{\sum_{\tilde{l} \in \mathcal{L}_k} |\hat{g}_{\tilde{l},k}|^2}. \quad (60)$$

Next, based on the results in *Theorem 2* and the relationship between the large-scale fading coefficients $\hat{\gamma}_{l,n}$ and $\gamma_{l,n}$ in (37), by applying *Lemma 2* in Appendix A to (60), we obtain

$$\mathbb{E}_{\mathbf{H}} \{ \|\hat{\mathbf{a}}_k\|_2^2 \} \approx \frac{1}{\hat{\Phi}_k (\hat{\Psi}_k - 1)}. \quad (61)$$

Finally, (55) is obtained by substituting (61) into (59) and simplifying. ■

Note that the expression in *Theorem 4* can be easily evaluated since it involves the pilot sequence power, uplink data power, and large-scale fading coefficients, as well as, the antenna index set \mathcal{L}_k . Interestingly, from (55), it is shown that the approximate lower-bound of the achievable uplink rate with imperfect CSI is similar as the perfect CSI in *Theorem 2*, since the the channel estimate error is involved that makes a little different. Moreover, when the pilot sequence power ρ_p becomes infinite, based on (37) and (38), $\tilde{\gamma}_{\max} \rightarrow 0$, $\hat{\Phi}_k \rightarrow \Phi_k$, $\hat{\Psi}_k \rightarrow \Psi_k$, and hence

$$\lim_{\rho_p \rightarrow \infty} \hat{R}_k^{\text{lb}} = \widetilde{R}_k^{\text{lb}}. \quad (62)$$

Moreover, with finite ρ_p , based on the monotonic property from (31), after some algebraic manipulation, it can be shown that $\widetilde{\hat{R}}_k^{\text{lb}} < \widetilde{R}_k^{\text{lb}}$. In a nutshell, $\widetilde{\hat{R}}_k^{\text{lb}}$ is very generic and can be regarded as a considered model to investigate the lower-bound performance of achievable uplink rate for the imperfect CSI case and its special case perfect CSI. Also, it is easy to show that $\widetilde{\hat{R}}_k^{\text{lb}} < \widetilde{\hat{R}}_k^{\text{ub}}$, which implies the validity of *Theorem 4*. Particularly, when $L \rightarrow \infty$, by taking the same assumption for obtaining (16), hence $\widetilde{\hat{R}}_k^{\text{lb}}$, after much algebraic manipulation, becomes

$$\widetilde{\hat{R}}_k^{\text{lb}} \rightarrow \log_2 \left(1 + \frac{\rho_u (L - K)}{\rho_u \sum_{n=1}^K \frac{\gamma_n}{\rho_p \gamma_n + 1} + 1} \times \frac{\rho_p \gamma_k}{\rho_p \gamma_k + 1} \gamma_k \right). \quad (63)$$

It is important to note that (63) is the exact lower-bound of the achievable uplink rate with ZF detector and imperfect CSI in the corresponding conventional massive MIMO system given by [16, Proposition 7]. Hence, $\widetilde{\hat{R}}_k^{\text{lb}}$ can be emerged as a promising, tractable, and effective expression to reap both benefits of the rate analysis of cell-free massive MIMO systems and conventional massive MIMO systems.

The following corollary presents an analysis for $\widetilde{\hat{R}}_k^{\text{lb}}$ by averaging out the large-scale fading coefficients. Few relative results can be found in the open literature based on the authors' knowledge.

Corollary 4: An lower-bound of $\widetilde{\hat{R}}_k$, $\widetilde{\hat{R}}_k^{\text{lb}}$, has the following approximation

$$\widetilde{\hat{R}}_k^{\text{lb}} \approx \widetilde{\hat{R}}_k^{\text{lb}} \triangleq \mathbb{E}_{\mathbf{r}} \left\{ \widetilde{\hat{R}}_k^{\text{lb}} \right\}. \quad (64)$$

Also, when $L \rightarrow \infty$, $\widetilde{\hat{R}}_k^{\text{lb}} = \Omega(\frac{\alpha}{2} \log_2 L)$.

Proof: Based on *Theorem 4*, it is easy to obtain the approximation (64). In the following, the asymptotic behaviour of $\widetilde{\hat{R}}_k^{\text{lb}}$ is proved.

First, by adopting the similar sorting method of large-scale fading coefficient and the methodology as in *Corollary 2*, as well as, the similar method for obtaining the inequality (51) in *Corollary 3*, $\widetilde{\hat{R}}_k^{\text{lb}}$ is lower-bounded by

$$\widetilde{\hat{R}}_k^{\text{lb}} > \mathbb{E}_{\mathbf{r}} \left\{ \log_2 \left(1 + \frac{\rho_u}{\rho_u \frac{K}{\rho_p} + 1} \hat{\gamma}_k^{(2)} \right) \right\} \triangleq \widetilde{\hat{R}}_k^{\text{lb-lb}}. \quad (65)$$

Next, by utilizing the similar way for obtaining (53) in *Corollary 3*, after much algebraic manipulation, furtherly, $\widetilde{\hat{R}}_k^{\text{lb-lb}}$ is lower-bounded by

$$\widetilde{\hat{R}}_k^{\text{lb-lb}} \geq \log_2 \left(1 + \frac{\rho_u \rho_p 2^{-\alpha}}{\left(\rho_u \frac{K}{\rho_p} + 1 \right) (\rho_p 2^{-\alpha} + 1) Q_2(L)} \right), \quad (66)$$

where the condition for reaching the “=” in “ \geq ” is the same as (33).

Finally, the asymptotic conclusion is obtained based on $Q_2(L) = \Theta(L^{-\frac{\alpha}{2}})$ in *Proposition 1* of Appendix A, (65), and (66). ■

Interestingly, comparison of *Corollary 3* and *Corollary 4* reveals that the obtained approximate bounds of the achievable uplink rate with ZF detector and imperfect CSI, have the same asymptotic lower-bound $\frac{\alpha}{2} \log_2 L$, which the same results can be found in *Corollary 1* and *Corollary 2* for the perfect CSI case. In other words, the channel estimation error introduced by the phase of channel estimation has no impact of the growth rate of the achievable uplink rate in cell-free massive MIMO systems. Also, in conventional massive MIMO systems with imperfect CSI, (49) and (63) show that the corresponding achievable uplink rate’s growth rate is just not more than $\log_2 L$ which is same as the perfect CSI case. Hence, cell-free massive MIMO systems also have the potential of high growth rate compared with the conventional massive MIMO systems in imperfect CSI. In the following section, all the above mentioned results will be examined completely based on the Monte-Carlo analogy.

V. NUMERICAL RESULTS

In this section, the validation of the theoretical analysis and asymptotic conclusion of the achievable uplink rate in Section III and Section IV is conducted via comparison with numerical simulation. Moreover, the impact of the pilot sequence power ρ_p is considered to investigate the achievable uplink rate performance. Specifically, by employing the methodology of [11, 16], we choose the path-loss factor $\alpha = 4$ and the number of users $K = 10$. The corresponding simulation results are obtained by uniformly and randomly producing 30 realizations of all users’ positions and 30 realizations of antennas positions in this circular area, respectively, with 200 realizations of the small-scale fading channels for each large-scale channel realization. For convenience, in this cell-free massive MIMO system, we define the metrics called “Average achievable uplink rate” for the perfect CSI case and imperfect CSI case, which are given by

$$\bar{R} \triangleq \frac{1}{K} \sum_{k=1}^K \bar{R}_k, \quad (67)$$

$$\bar{\bar{R}} \triangleq \frac{1}{K} \sum_{k=1}^K \bar{\bar{R}}_k, \quad (68)$$

respectively. Also, \bar{R}_k and $\bar{\bar{R}}_k$ have been defined as in (9) and (43), respectively. Moreover, for further comparison, the conventional massive MIMO system is considered in this section, which

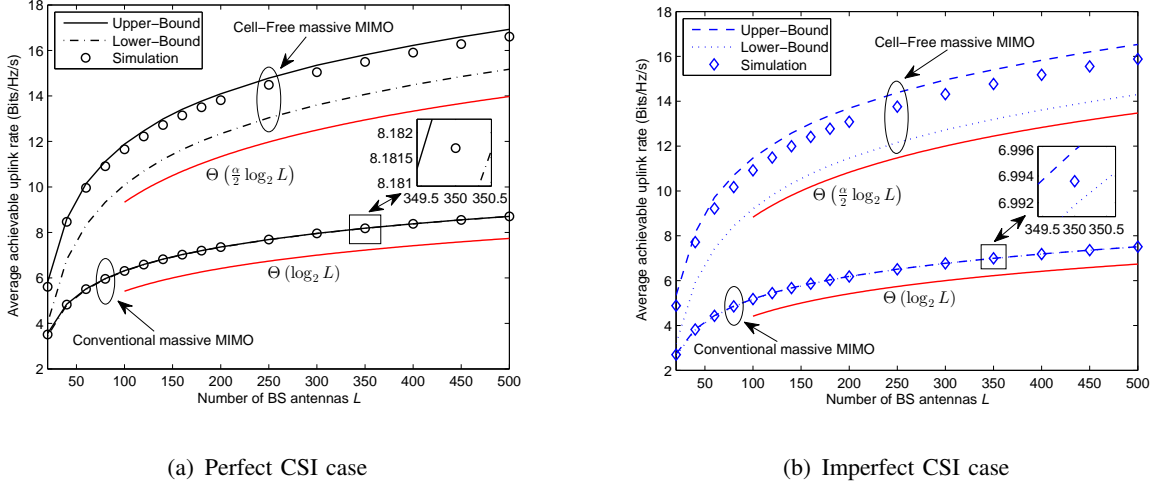


Fig. 2. The average achievable uplink rate as a function of the number of BS antennas L with the common parameter $\rho_u = -10\text{dB}$ for both cell-free massive MIMO system and conventional massive MIMO system based on the perfect CSI case and imperfect CSI case ($\rho_p = 0\text{dB}$), respectively.

the corresponding parameter setting and metric are the same as in the cell-free massive MIMO system except all the BS antennas are placed and fixed at this circular area centre.

Fig. 2 gives the analytical upper-bound, lower-bound, and Monte-Carlo simulated average achievable uplink rate with the cell-free massive MIMO system and conventional massive MIMO system, respectively. All results are shown for $\rho_u = -10\text{dB}$ and also the imperfect CSI results are based on the parameter $\rho_p = 0\text{dB}$.²

For the perfect CSI case of Fig. 2 (a), with the cell-free massive MIMO system, it is shown that, compared with the simulated average achievable uplink rate curve, the obtained upper-bound (based on (11) and (17)) and lower-bound (based on (20) and (27)) curves are effective, tight, and have the similar growth rate. In other words, it justifies the effectiveness of *Theorem 1* and *Theorem 2*. The similar results can also be found for the conventional massive MIMO system, which the upper-bound and lower-bound curves are based on averaging out the large-scale fading in the results (16) and (26), respectively. Also, it is found that as the number of BS antennas increases, the gap between these two systems is gradually increased for all obtained bounds and simulated rate, which shows the cell-free massive MIMO system has a huge development potential for achievable uplink rate improving. Moreover, to explore and

²Since we assume that the noise variance is 1, ρ_u (ρ_p) can be interpreted as the transmit uplink data signal (pilot sequence signal) to noise ratio and, thus, can be expressed in dB.

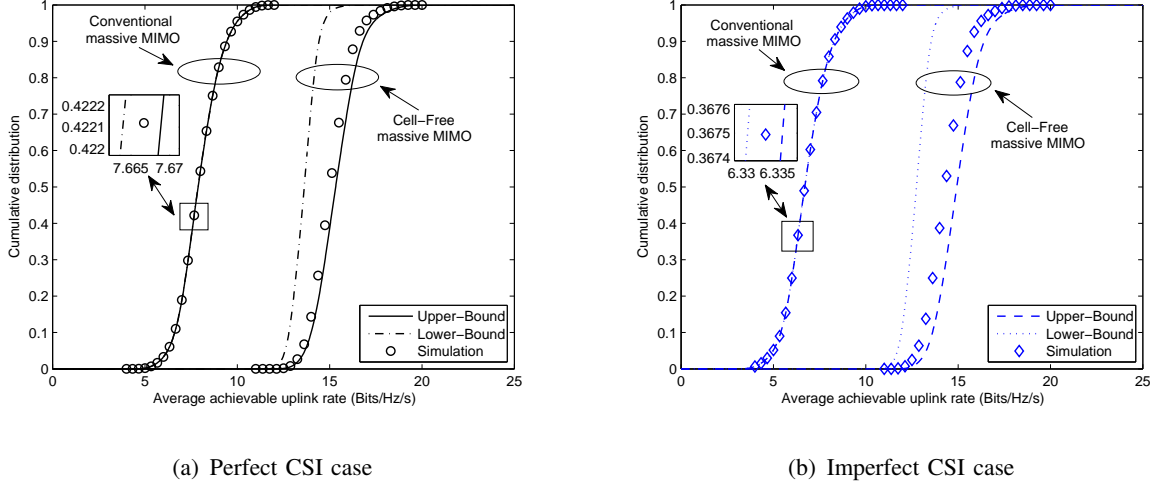


Fig. 3. The CDF of the average achievable uplink rate with the common parameters $L = 300$ and $\rho_u = -10\text{dB}$ for both cell-free massive MIMO system and conventional massive MIMO system based on the perfect CSI case and imperfect CSI case ($\rho_p = 0\text{dB}$), respectively.

analyze the scaling behaviour of the achievable uplink rate, two numerical curves which have the asymptotic properties $\Theta\left(\frac{\alpha}{2} \log_2 L\right)$ and $\Theta(\log_2 L)$, respectively, are also plotted.³ Compared with these two numerical curves, it is shown that, for the cell-free massive MIMO system, the corresponding bounds and simulated rate have an asymptotic lower-bound $\frac{\alpha}{2} \log_2 L$ as $L \rightarrow \infty$ which prove the validity of *Corollary 1* and *Corollary 2*; for the conventional massive MIMO system, the corresponding bounds and simulated rate do have an asymptotically tight bound $\log_2 L$ which satisfies the conclusion of the discussion after *Corollary 2*.

For the imperfect CSI case of Fig. 2 (b), the upper-bound and lower-bound curves in cell-free massive MIMO system are based on (44) with (50), and (55) with (64), respectively, while the upper-bound and lower-bound curves in conventional massive MIMO system are based on averaging out the large-scale fading in the results (49) and (63), respectively. It is found that the above mentioned observations in perfect CSI case can also be found in imperfect CSI case, which prove the validity of *Theorem 3*, *Theorem 4*, *Corollary 3*, *Corollary 4*, and conclusion of the discussion after *Corollary 4*. Only the achievable uplink rate-loss is introduced into the imperfect CSI case for both two systems.

³To avoid confusion, the detailed parameters of these two curves has not been provided since the provided asymptotic properties are enough. We also apply this methodology in Fig. 2 (b).

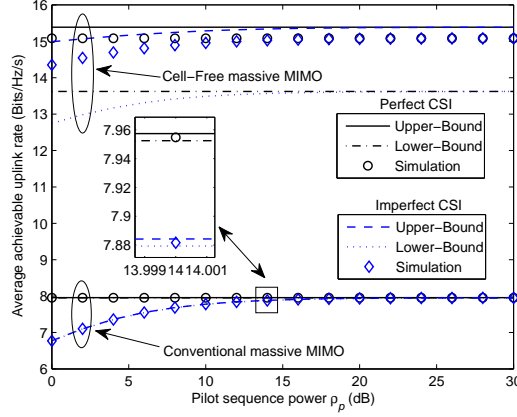


Fig. 4. The average achievable uplink rate as a function of the pilot sequence power ρ_p with the parameters $\rho_u = -10\text{dB}$ and $L = 300$ for both the perfect CSI case and imperfect CSI case, in cell-free massive MIMO system and conventional massive MIMO system, respectively.

Fig. 3 presents the cumulative distribution function (CDF) of the average achievable uplink rate with $\rho_u = -10\text{dB}$ and the cell-free massive MIMO system, as well as, the conventional massive MIMO system, for perfect CSI case and imperfect CSI case ($\rho_p = 0\text{dB}$), under the setting of the number of BS antennas is equal to 300. Also, the corresponding bound results are offered for comparison. Specifically, for the perfect CSI case of Fig. 3 (a), for the cell-free massive MIMO system, the upper-bound curve and the lower-bound curve line at the either end of the exact simulated achievable uplink rate curve for the whole rate region, and the upper-bound is tight compared with the simulation result, which imply that the obtained analytical results in the perfect CSI case are valid for the whole CDF region. Moreover, compared with the conventional massive MIMO system, not only the bound results, but also the simulation result shows huge advantage in regard of the rate metric. For the imperfect CSI case of Fig. 3 (b), again, the above mentioned observations in perfect CSI case can also be deduced that obtained analytical results in the imperfect CSI case are very effective and only achievable uplink rate loss is inevitable due to the channel estimation error.

Fig. 4 investigates the impact of the pilot sequence power ρ_p on the average achievable uplink rate performance. In this figure, the uplink data power is set to -10dB and the number of BS antennas is set to 300. For the cell-free massive MIMO system, it shows that the analytical upper-bound and lower-bound values are effective regardless of the value of ρ_p compared with simulation values for both perfect CSI and imperfect CSI cases. Also, the obtained lower-bound

has the similar growth rate with the exact simulated rate in imperfect CSI case. Moreover, when $\rho_p \rightarrow \infty$, the upper-bound, lower-bound, and simulated rate for imperfect CSI case approach to different constant values, which match the upper-bound, lower-bound, and simulated rate for perfect CSI case, respectively. In other words, those results showcase the conclusions of (48) and (62) that the performance of imperfect CSI case is always less than the perfect CSI case. The above mentioned results can also be found in the conventional massive MIMO system in this figure. Moreover, from this figure, for different ρ_p , the corresponding performance of cell-free massive MIMO system is far better than the conventional massive MIMO system.

VI. CONCLUSION

The SE properties of the cell-free massive MIMO systems are of high practical importance for system design, as well as, other applications. However, few references have been reported on their analytical analysis based on the tractable, relatively accurate, and insightful SE expressions. Under this background, in this paper, we presented a seminal study for investigating the achievable uplink rate performance of cell-free massive MIMO systems employing ZF detectors, yielding the simple but powerful approximate closed-form bound results applying for the perfect CSI case and imperfect CSI case, respectively. To demonstrate the utility of the seminal study, in the first part of the paper, the system structure, channel model, and uplink data transmission were briefly introduced. In the second part of the paper, we had considered the upper-bound and lower-bound of the achievable uplink rate with perfect CSI for which the novel approximate expressions were deduced. Also, the obtained analytical bounds can degrade into the exact bound results in the conventional massive MIMO systems. Particularly, by averaging out the large-scale fading, through those bound expressions, we obtained key insights into the effect of the *distance diversity* offered by the cell-free massive MIMO systems. It was found that, at high number of BS antennas L , the upper-bound and lower-bound by averaging out the large-scale fading had the asymptotic lower-bound $\frac{\alpha}{2} \log_2 L$, whilst for the bound results in conventional massive MIMO systems, it had the asymptotically tight bound $\log_2 L$. In other words, those asymptotic results showed the potential of cell-free massive MIMO systems since the path-loss factor $\alpha > 2$ except the free space environment. In the third part of the paper, the imperfect CSI was involved in the analysis of the achievable uplink rate. The above mentioned conclusions in perfect CSI case were also true of the imperfect CSI case but with a little bit rate loss. In addition, the obtained

bounds results in imperfect CSI case degraded into the perfect CSI case when pilot sequence power ρ_p became infinite.

APPENDIX A SEVERAL USEFUL RESULTS

Lemma 1 ([10, Eqs. (57-59)], [24, Eqs. (43-46)], and [37, Eq. (3.1)]: Consider a circular area with unit radius, user k and $L - K + 1$ ($L > K - 1$) antennas are uniformly distributed within this area. ρ_k denotes the distance between user k and the circular area centre. The PDF of ρ_k is given by

$$f_{\rho_k}(x) \triangleq 2x, 0 \leq x \leq 1. \quad (69)$$

Let $d_k^{(l)}$ ($l = 1, \dots, L - K + 1$) is the l th minimum access distance from user k to the $L - K + 1$ antennas, which its conditional PDF given ρ_k is

$$f_{d_k^{(l)}|\rho_k}(y|x) \triangleq \frac{(L-K+1)!}{(l-1)!(L-K+1-l)!} (F(y;x))^{l-1} (1-F(y;x))^{L-K+1-l} f(y;x), 0 \leq y \leq 1+x, \quad (70)$$

where $F(y;x)$ and $f(y;x)$ denote the CDF and the PDF of the access distance from user k to any antenna, which are defined as

$$F(y;x) \triangleq \begin{cases} y^2, & 0 \leq y \leq 1-x, \\ \frac{y^2}{\pi} \arccos \frac{x^2+y^2+1}{2xy} + \frac{1}{\pi} \arccos \frac{1+x^2-y^2}{2x} - \frac{2}{\pi} S_{\Delta}(x,y), & 1-x < y \leq 1+x, \end{cases} \quad (71)$$

and

$$f(y;x) \triangleq \begin{cases} 2y, & 0 \leq y \leq 1-x, \\ \frac{2y}{\pi} \arccos \frac{x^2+y^2+1}{2xy}, & 1-x < y \leq 1+x, \end{cases} \quad (72)$$

respectively. Also, $S_{\Delta}(x,y)$ is defined as

$$S_{\Delta}(x,y) \triangleq \sqrt{\frac{x+y+1}{2} \left(\frac{x+y+1}{2} - 1 \right) \left(\frac{x+y+1}{2} - x \right) \left(\frac{x+y+1}{2} - y \right)}. \quad (73)$$

Lemma 2 ([13, Lemma 2] and [38, Lemma 6 & Proposition 8]): If X_l ($l = 1, \dots, L$) is an independent Gamma distributed random variable with a shape parameter η_l and a scale parameter θ_l , i.e., $X_l \sim \Gamma(\eta_l, \theta_l)$, then, the sum random variable $X = \sum_{l=1}^L X_l$ can be approximated by a Gamma distributed random variable $\hat{X} \sim \Gamma(\hat{\eta}, \hat{\theta})$, which $\hat{\eta}$ and $\hat{\theta}$ are defined as $\hat{\eta} \triangleq \left(\sum_{l=1}^L \eta_l \theta_l \right)^2 / \sum_{l=1}^L \eta_l \theta_l^2$ and $\hat{\theta} \triangleq \sum_{l=1}^L \eta_l \theta_l^2 / \sum_{l=1}^L \eta_l \theta_l$, respectively.

Proposition 1: Consider the same conditions as in *Lemma 1*, for fixed l , as $L \rightarrow \infty$, the expectation of $\left(d_k^{(l)}\right)^\alpha$ has the following asymptotic property⁴

$$Q_l(L) \triangleq \mathbb{E}_{d_k^{(l)}} \left\{ \left(d_k^{(l)}\right)^\alpha \right\} = \Theta \left(L^{-\frac{\alpha}{2}} \right), \quad (74)$$

where α is the path-loss factor which satisfies $\alpha > 2$ except the free space environment.

Proof: Based on the definition of the expectation, we start by writing

$$Q_l(L) = \int_0^1 f_{\rho_k}(x) dx \int_0^{1+x} f_{d_k^{(l)}|\rho_k}(y|x) y^\alpha dy. \quad (75)$$

To evaluate the integral (75), by substituting (70) into $Q_l(L)$ and defining $z \triangleq F(y; x)$, after some algebraic manipulation, we have

$$Q_l(L) = \frac{(L - K + 1)!}{(l - 1)!(L - K + 1 - l)!} \int_0^1 f_{\rho_k}(x) dx \overbrace{\int_0^1 z^{l-1} (1 - z)^{L-K+1-l} \left(F^{-1}(z; x)\right)^\alpha dz}^{Q_l(L; x)}, \quad (76)$$

where $F^{-1}(\cdot)$ denotes the inverse function of $F(\cdot)$.

To analyze the scaling behavior of $Q_l(L)$, we firstly investigate the term $Q_l(L; x)$. Based on the structure of $F(y; x)$ in (71), when $0 \leq y \leq 1 - x$, we denote $F(y; x)$ as $F_1(y; x)$. When $1 - x < y \leq 1 + x$, we denote $F(y; x)$ as $F_2(y; x)$. Hence, for the term $Q_l(L; x)$, after much algebraic manipulation, we perform the following sequence of operations as

$$\begin{aligned} Q_l(L; x) &= \underbrace{\int_0^1 z^{l-1} (1 - z)^{L-K+1-l} \left(F_1^{-1}(z; x)\right)^\alpha dz}_{Q_{l1}(L; x)} \\ &\quad + \underbrace{\int_{(1-x)^2}^1 z^{l-1} (1 - z)^{L-K+1-l} \left(\left(F_2^{-1}(z; x)\right)^\alpha - \left(F_1^{-1}(z; x)\right)^\alpha \right) dz}_{Q_{l2}(L; x)}. \end{aligned} \quad (77)$$

Note that, based on the geometrical relationship in [10, Fig. 14] and (71), when $0 < x \leq 1$ and $\forall z \in ((1 - x)^2, 1]$, it is obvious that

$$\pi \left(\frac{F_2^{-1}(z; x) + (1 - x)}{2} \right)^2 \leq \pi z < \pi \left(F_2^{-1}(z; x) \right)^2, \quad (78)$$

where the “=” in “ \leq ” is reached when $z = 1$. Then (78) yields

$$1 - x < F_1^{-1}(z; x) < F_2^{-1}(z; x) \leq 2F_1^{-1}(z; x) - (1 - x). \quad (79)$$

⁴Note that the specifical case $l = 1$ has been provided in [11] with brief proof. Here, we provide detailed result for general case which is very generic.

Hence, with the aid of (79), when $0 < x \leq 1$, the term $Q_{l2}(L; x)$ is upper-bounded by

$$Q_{l2}(L; x) < (2^\alpha - 1) \int_{(1-x)^2}^1 z^{l-1} (1-z)^{L-K+1-l} (F_1^{-1}(z; x))^\alpha dz < (2^\alpha - 1) Q_{l1}(L; x). \quad (80)$$

Moreover, when $x = 0$, $Q_{l2}(L; 0) = 0$ and $Q_{l1}(L; 0) > 0$. Hence, it is proved that

$$Q_{l2}(L; x) = O(Q_{l1}(L; x)), \forall x \in [0, 1]. \quad (81)$$

Next, based on (71), the integral $Q_{l1}(L; x)$ is now evaluated as

$$Q_{l1}(L; x) = \int_0^1 z^{l+\frac{\alpha}{2}-1} (1-z)^{L-K+1-l} dz = B\left(l + \frac{\alpha}{2}, L - K + 1 - (l - 1)\right), \quad (82)$$

where $B(x, y) \triangleq \int_0^1 t^{x-1} (1-t)^{y-1} dt$ is the Beta function. Note that when y is large and x is fixed, $B(x, y) \rightarrow \Gamma(x) y^{-x}$, hence when $L \rightarrow \infty$, we have

$$Q_{l1}(L; x) \rightarrow \frac{\Gamma(l + \frac{\alpha}{2})}{(L - K + 1 - (l - 1))^{l+\frac{\alpha}{2}}} = \Theta(L^{-(l+\frac{\alpha}{2})}). \quad (83)$$

Then, based on (81) and (83), we have

$$Q_l(L; x) = \Theta(L^{-(l+\frac{\alpha}{2})}). \quad (84)$$

Finally, the conclusion (74) is obtained by substituting (84) into (76) and simplifying. ■

ACKNOWLEDGMENT

The authors would like to thank Dr. Lin Dai, from City University of Hong Kong, for her generous help in improving this paper.

REFERENCES

- [1] Qualcomm, "The 1000x data challenge," [Online]. Available: <https://www.qualcomm.com/1000x>
- [2] T. L. Marzetta, "Noncooperative cellular wireless with unlimited numbers of base station antennas," *IEEE Trans. Wireless Commun.*, vol. 9, no. 11, pp. 3590-3600, Nov. 2010.
- [3] F. Boccardi, R. W. Heath, Jr., A. Lozano, T. L. Marzetta, and P. Popovski, "Five disruptive technology directions for 5G," *IEEE Commun. Mag.*, vol. 52, no. 2, pp. 74-80, Feb. 2014.
- [4] T. L. Marzetta, E. G. Larsson, H. Yang, and H. Q. Ngo, *Fundamentals of Massive MIMO*. Cambridge, U.K.: Cambridge Univ. Press, 2016.
- [5] P. Liu, S. Jin, T. Jiang, Q. Zhang, and M. Matthaiou, "Pilot power allocation through user grouping in multi-cell massive MIMO systems," *IEEE Trans. Commun.*, vol. 65, no. 4, pp. 1561-1574, Apr. 2017.
- [6] C. Zhang, Y. Jing, Y. Huang, and L. Yang, "Performance analysis for massive MIMO downlink with low complexity approximate zero-forcing precoding," *IEEE Trans. Commun.*, 2018, to appear. [Online]. Available: <https://arxiv.org/abs/1711.00415>
- [7] S. Qiu, D. Chen, D. Qu, K. Luo, and T. Jiang, "Downlink precoding with mixed statistical and imperfect instantaneous CSI for massive MIMO systems," *IEEE Trans. Veh. Technol.*, vol. 67, no. 4, pp. 3028-3041, Apr. 2018.

- [8] M. Feng, S. Mao, and T. Jiang, "BOOST: Base station on-off switching strategy for green massive MIMO HetNets," *IEEE Trans. Wireless Commun.*, vol. 16, no. 11, pp. 7319-7332, Sept. 2017.
- [9] A. A. M. Saleh, A. J. Rustako, and R. S. Roman, "Distributed antennas for indoor radio communications," *IEEE Trans. Commun.*, vol. 35, no. 12, pp. 1245-1251, Dec. 1987.
- [10] L. Dai, "A comparative study on uplink sum capacity with co-located and distributed antennas," *IEEE J. Sel. Areas Commun.*, vol. 29, no. 6, pp. 1200-1213, Jun. 2011.
- [11] —, "An uplink capacity analysis of the distributed antenna system (DAS): From cellular DAS to DAS with virtual cells," *IEEE Trans. Wireless Commun.*, vol. 13, no. 5, pp. 2717-2731, May 2014.
- [12] H. Q. Ngo, A. Ashikhmin, H. Yang, E. G. Larsson, and T. L. Marzetta, "Cell-free massive MIMO versus small cells," *IEEE Trans. Wireless Commun.*, vol. 16, no. 3, pp. 1834-1850, Mar. 2017.
- [13] J. Li, D. Wang, P. Zhu, J. Wang, and X. You, "Downlink spectral efficiency of distributed massive MIMO systems with linear beamforming under pilot contamination," *IEEE Trans. Veh. Technol.*, vol. 67, no. 2, pp. 1130-1145, Feb. 2018.
- [14] E. Telatar, "Capacity of multi-antenna Gaussian channels," *Euro. Trans. Telecommun.*, vol. 10, no. 6, pp. 585-595, Nov.-Dec. 1999.
- [15] A. M. Tulino and S. Verdú, "Random matrix theory and wireless communications," *Found. Trends Commun. Inf. Theory*, vol. 1, no. 1, pp. 1-182, Jun. 2004.
- [16] H. Q. Ngo, E. G. Larsson, and T. L. Marzetta, "Energy and spectral efficiency of very large multiuser MIMO systems," *IEEE Trans. Commun.*, vol. 61, no. 4, pp. 1436-1449, Apr. 2013.
- [17] N. Auguin, D. Morales-Jimenez, and M. R. McKay, "Exact statistical characterization of 2×2 Gram matrices with arbitrary variance profile," *IEEE Trans. Veh. Technol.*, vol. 66, no. 9, pp. 8575-8579, Sept. 2017.
- [18] J. Li, D. Wang, P. Zhu, and X. You, "Spectral efficiency analysis of single-cell multi-user large-scale distributed antenna system," *IET Commun.*, vol. 8, no. 12, pp. 2213-2221, Aug. 2014.
- [19] Z. D. Bai and J. W. Silverstein, *Spectral Analysis of Large Dimensional Random Matrices*, 2nd ed. Springer Series in Statistics, New York, NY, USA, 2009.
- [20] B. Hassibi and B. M. Hochwald, "How much training is needed in multiple-antenna wireless links?" *IEEE Trans. Inf. Theory*, vol. 49, no. 4, pp. 951-963, Apr. 2003.
- [21] N. Akbar, E. Björnson, E. G. Larsson, and N. Yang, "Downlink power control in massive MIMO networks with distributed antenna arrays," *IEEE ICC*, 2018, to appear. [Online]. Available: <https://arxiv.org/abs/1801.07862>
- [22] J. Zuo, J. Zhang, C. Yuen, W. Jiang, and W. Luo, "Energy-efficient downlink transmission for multicell massive DAS with pilot contamination," *IEEE Trans. Veh. Technol.*, vol. 66, no. 2, pp. 1209-1221, Feb. 2017.
- [23] L. Li, D. Wang, P. Zhu, and X. You, "Benefits of beamforming training scheme in distributed large-scale MIMO systems," *IEEE Access*, vol. 6, pp. 7432-7444, 2018.
- [24] J. Wang and L. Dai, "Asymptotic rate analysis of downlink multi-user systems with co-located and distributed antennas," *IEEE Trans. Wireless Commun.*, vol. 14, no. 6, pp. 3046-3058, Jun. 2015.
- [25] M. Bashar, K. Cumanan, A. G. Burr, M. Debbah, and H. Q. Ngo, "Enhanced max-min SINR for uplink cell-free massive MIMO systems," *IEEE ICC*, 2018, to appear. [Online]. Available: <https://arxiv.org/abs/1801.10188>
- [26] E. Nayebi, A. Ashikhmin, T. L. Marzetta, H. Yang, and B. D. Rao, "Precoding and power optimization in cell-free massive MIMO systems," *IEEE Trans. Wireless Commun.*, vol. 16, no. 7, pp. 4445-4459, Jul. 2017.
- [27] T. X. Doan, H. Q. Ngo, T. Q. Duong, and K. Tourki, "On the performance of multigroup multicast cell-free massive MIMO," *IEEE Commun. Lett.*, vol. 21, no. 12, pp. 2642-2645, Dec. 2017.
- [28] G. Interdonato, H. Q. Ngo, E. G. Larsson, and P. Frenger, "How much do downlink pilots improve cell-free massive MIMO?" in *Proc. IEEE GLOBECOM*, Dec. 2016.

- [29] H. Q. Ngo, L.-N. Tran, T. Q. Duong, M. Matthaiou, and E. G. Larsson, "On the total energy efficiency of cell-free massive MIMO," *IEEE Trans. Green Commun. Netw.*, vol. 2, no. 1, pp. 25-39, Mar. 2018.
- [30] H. B. Almelah and K. A. Hamdi, "Spectral efficiency of distributed large-scale MIMO systems with ZF receivers," *IEEE Trans. Veh. Technol.*, vol. 66, no. 6, pp. 4834-4844, Jun. 2017.
- [31] A. Yang, Y. Jing, C. Xing, Z. Fei, and J. Kuang, "Performance analysis and location optimization for massive MIMO systems with circularly distributed antennas," *IEEE Trans. Wireless Commun.*, vol. 14, no. 10, pp. 5659-5671, Oct. 2015.
- [32] L. D. Nguyen, T. Q. Duong, H. Q. Ngo, and K. Tourki, "Energy efficiency in cell-free massive MIMO with zero-forcing precoding design," *IEEE Commun. Lett.*, vol. 21, no. 8, pp. 1871-1874, Aug. 2017.
- [33] T. H. Cormen, C. E. Leiserson, R. L. Rivest, and C. Stein, *Introduction to Algorithms*, 3rd ed. Cambridge, MA, USA: MIT Press, 2009.
- [34] Q. Zhang, S. Jin, M. R. McKay, D. Morales-Jimenez, and H. Zhu, "Power allocation schemes for multicell massive MIMO systems," *IEEE Trans. Wireless Commun.*, vol. 14, no. 11, pp. 5941-5955, Nov. 2015.
- [35] S. M. Kay, *Fundamentals of Statistical Signal Processing: Estimation Theory*. Prentice-Hall, Inc. Upper Saddle River, NJ, USA, 1993.
- [36] X. Wang, Y. Wang, and S. Ma, "Upper bound on uplink sum rate for multi-cell massive MU-MIMO systems with ZF receivers," *IEEE Wireless Commun. Lett.*, vol. 6, no. 2, pp. 250-253, Apr. 2017.
- [37] H.-C. Yang and M.-S. Alouini, *Order Statistics in Wireless Communications: Diversity, Adaptation, and Scheduling in MIMO and OFDM Systems*. Cambridge, U.K.: Cambridge Univ. Press, 2011.
- [38] R. W. Heath, Jr., T. Wu, Y. H. Kwon, and A. C. K. Soong, "Multiuser MIMO in distributed antenna systems with out-of-cell interference," *IEEE Trans. Signal Process.*, vol. 59, no. 10, pp. 4885-4899, Oct. 2011.